Cell PRESS
Open ACCESS

Cell Reports
Article

Luminal Iron Levels Govern Intestinal Tumorigenesis after *Apc* Loss In Vivo

Sorina Radulescu,[1] Matthew J. Brookes,[2] Pedro Salgueiro,[1] Rachel A. Ridgway,[1] Ewan McGhee,[1] Kurt Anderson,[1] Samuel J. Ford,[2] Daniel H. Stones,[2] Tariq H. Iqbal,[2] Chris Tselepis,[2,*] and Owen J. Sansom[1,*]
[1]Beatson Institute of Cancer Research, Glasgow, G61 1BD, UK
[2]Birmingham Cancer Research UK Centre, School of Cancer Sciences, University of Birmingham B15 2TH, UK
*Correspondence: c.tselepis@bham.ac.uk (C.T.), o.sansom@beatson.gla.ac.uk (O.J.S.)
http://dx.doi.org/10.1016/j.celrep.2012.07.003

SUMMARY

It is clear from epidemiological studies that excess iron is associated with increased risk of colorectal cancer; however, questions regarding the mechanism of how iron increases cancer risk, the source of the excess iron (circulating or luminal), and whether iron reduction represents a potential therapeutic option remain unanswered. In this study, we show that after *Apc* deletion, the cellular iron acquisition proteins TfR1 and DMT1 are rapidly induced. Conversely, restoration of APC reduces cellular iron due to repression of these proteins. To test the functional importance of these findings, we performed in vivo investigations of the impact of iron levels on intestinal tumorigenesis. Strikingly, depletion of luminal (but not systemic) iron strongly suppressed murine intestinal tumorigenesis, whereas increased luminal iron strongly promoted tumorigenesis. Taken together, our data definitively delineate iron as a potent modifier of intestinal tumorigenesis and have important implications for dietary iron supplementation in patients at high risk of colorectal cancer.

INTRODUCTION

The *Apc* (adenomatous polyposis coli) gene is the most commonly mutated tumor suppressor gene in sporadic colorectal cancer (CRC; Bienz and Clevers, 2000). Loss of the APC protein prevents the turnover of β-catenin, and hence β-catenin accumulates in the nucleus and causes the activation of TCF/LEF or Wnt target genes such as *c-Myc* and *Cyclin D2* (Bienz and Clevers, 2000). Of importance, APC loss appears to initiate CRC, and thus one would predict that agents that can determine the survival of APC-deficient cells could potently modify tumor risk. In this context, a number of epidemiological studies have shown that dietary factors can alter CRC risk (World Cancer Research Fund / American Institute for Cancer Research, 2011). However, whether these agents target APC-deficient cells over normal cells, as well as their mechanism of action, is still unclear.

Iron is essential for all organisms, and iron-containing proteins catalyze a variety of crucial metabolic processes, such as oxidative phosphorylation and DNA synthesis, as well as cell-cycle progression and growth (Le and Richardson, 2002). In addition, excess iron can mediate reactive oxygen species through Fenton reaction chemistry, resulting in lipid, protein, and DNA damage (Toyokuni, 1996). A link between excess iron and cancer incidence in CRC has been reported (Chua et al., 2010; Kato et al., 1999; Lee et al., 2004; Mainous et al., 2005; Nelson, 2001; Toyokuni, 2009; Weinberg, 1994, 1996). Most notably, a meta-analysis of 33 epidemiological studies showed that 75% of studies supported an association between excess iron and CRC risk (Nelson, 2001). This is supported by the observation that patients with hemochromatosis (*HFE*) mutations, associated with the iron overload disorder hereditary hemochromatosis, have an increased risk of not only hepatocellular carcinoma but also CRC (Nelson et al., 1995; Shaheen et al., 2003). Conversely, several human epidemiological studies showed that a decrease in total body iron levels resulting from blood withdrawal decreases the risk of various cancers, including CRC (Edgren et al., 2008; Zacharski et al., 2008). However, despite this close association with tumorigenesis and disease, the role of iron in sporadic carcinogenesis and the mechanism by which it acts are still unclear. In particular, whether iron levels are a cause or a side effect of tumorigenesis has yet to be established, with previous studies in animal models reporting conflicting evidence regarding the impact of iron on colon cells (Lund et al., 1998; Soyars and Fischer, 1998).

Our own previous studies demonstrated that stimulating colorectal cell lineages with iron results in amplification of Wnt signaling (Brookes et al., 2008), the major oncogenic signaling pathway in the colon (Bienz and Clevers, 2000). Of importance, though, iron could only amplify Wnt signaling in the background of a loss of the tumor suppressor APC. These observations were further supported by a more recent study that highlighted a class of iron chelators (acyl hydrazones) as inhibitors of Wnt signaling and cell growth (Song et al., 2011). Furthermore, we previously reported a modulation in the expression of iron transport proteins in the malignant progression of disease (Brookes et al., 2006; Ward et al., 2008). In particular, in the process of human CRC, there was increased expression of the cellular iron

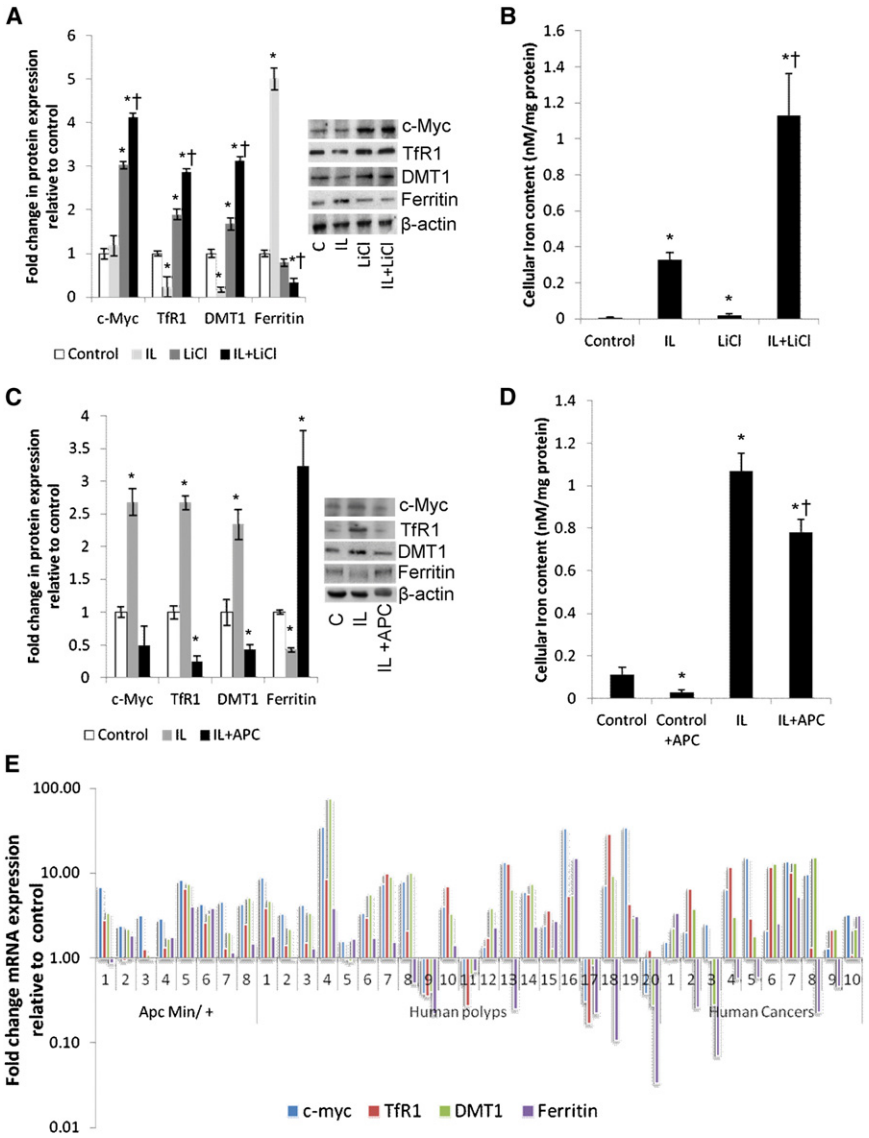

Figure 1. Effect of Modulating Wnt Signaling on Expression of Iron Transport Proteins

(A) Culturing RKO cells with iron (IL) for 24 hr repressed TfR1 and DMT1, and increased ferritin protein levels. LiCl treatment increased the level of TfR1, DMT1, and c-Myc expression relative to control. Costimulation with LiCl and IL (IL+LiCl) further increased c-MYC, TfR1, and DMT1 levels and suppressed ferritin expression. $p < 0.0001$ c-MYC, DMT1, $p = 0.0071$ TfR1 in IL+LiCl versus IL alone; $p = 0.003$ c-MYC, $p = 0.0017$ TfR1, $p = 0.0007$ DMT1 in IL+LiCl versus LiCl alone, Student's t test; * denotes statistical significance compared with control; † denotes statistical significance compared with LiCl alone. β-actin was used for protein normalization. Data are presented as mean ± SEM.

(B) To assess cellular IL levels, a ferrozine assay was performed in RKO cells in control or in the presence of IL or LiCl, or both (IL+LiCl) for 24 hr. Wnt activation further increases IL content ($p < 0.0001$ IL+LiCl versus LiCl alone, $p = 0.0006$ IL+LiCl versus IL alone, Student's t test; * denotes statistical significance compared with control; † denotes statistical significance compared with LiCl alone). Data are presented as mean ± SEM.

(C) Culturing SW480 cells for 24 hr with IL resulted in upregulation of c-MYC, TfR1, and DMT1, and repression of ferritin. Reconstitution of WT human Apc and culture with IL (IL+APC) significantly reduced c-MYC, TfR1 and DMT1 and ferritin expression ($p = 0.002$ TfR1, $p = 0.003$ DMT1, $p < 0.0001$ ferritin IL+APC versus IL, Student's t test; * denotes statistical significance compared with control). Data are presented as mean ± SEM.

(D) SW480 cells reconstituted with WT human APC resulted in significantly decreased cellular IL content (ferrozine assay; control+APC versus control, $p = 0.0053$; control+APC versus IL +APC, $p < 0.0048$, Student's t test; * denotes statistical significance compared with control; † denotes statistical significance compared with IL alone). Data are presented as mean ± SEM.

(E) To assess the association of c-MYC with TfR1, DMT1, and ferritin in vivo, mRNA expression levels were assessed in eight murine polyps from individual $Apc^{Min/+}$ mice, 20 human colonic polyps, and 10 human colorectal carcinomas. Expression levels were assessed relative to matched normal control mucosa.

import proteins (transferrin receptor 1 (TfR1) and divalent metal transporter 1 (DMT1), and a loss of cellular iron export function.

Although both the epidemiological evidence and results from our human cell line mechanistic studies are suggestive of a direct role of iron in CRC, it should be remembered that 25% of epidemiological studies have failed to find a link with iron consumption, and the increase in relative risk, although significant, is small. Thus, it is vital to test for a direct role of iron in sporadic carcinogenesis in vivo. In this study, we investigate how iron modulation affects intestinal tumorigenesis following Apc loss in vivo. Of importance, we show that the precise levels of iron dictate the proliferation and survival of *Apc*-deficient cells. This directly translates to suppressed tumorigenesis when luminal iron is depleted, and to increased tumorigenesis when luminal iron is in excess.

RESULTS

Modulation of Iron Transport Proteins as a Consequence of Wnt Signaling

To ascertain whether the expression of the iron import proteins TfR1 and DMT1, and the iron storage protein ferritin are modulated as a consequence of Wnt signaling, we selected and cultured two cell lines, RKO and SW480, in the presence and absence of iron. These two lines were chosen because they contain wild-type (WT) and mutant *Apc*, respectively. By activating Wnt signaling [via GSK3β inhibition using lithium chloride (LiCl)] in RKO cells, a 3-fold c-MYC induction was also associated with significant increases in TfR1 (mean 1.8-fold, $p = 0.021$) and DMT1 (mean 1.7-fold, $p = 0.036$) protein expression compared with control (Figure 1A). No change was

observed for ferritin protein expression. Costimulation of cells with the GSK3β inhibitor and iron further enhanced c-MYC, TfR1, and DMT1 levels by at least one-third above either GSK3 inhibitor or iron alone ($p < 0.0001$ c-MYC, DMT1; $p = 0.0071$ TfR1 in iron+LiCl versus iron alone; $p = 0.003$ c-MYC; $p = 0.0017$ TfR1; $p = 0.0007$ DMT1 in iron+LiCl versus LiCl alone; Figure 1A). Conversely, ferritin protein expression was statistically repressed by half or more compared with either GSK3 inhibitor ($p = 0.013$) or iron alone ($p = 0.02$). Of interest, without GSK3 inhibition, there was a dramatic decrease in TfR1 and DMT1 following treatment with iron, which was not observed following the activation of Wnt signaling ($p < 0.0001$). This made an important functional difference because when Wnt signaling was activated, the cells were now able to increase the expression of their cellular iron import proteins. This was evidenced by increased cellular iron deposition in cells challenged with iron and LiCl compared with cells challenged with iron (mean 3-fold, $p = 0.0003$) or LiCl alone (mean 40-fold, $p < 0.0001$; Figure 1B). To further solidify these observations, we performed a reverse set of experiments in which the expression of c-MYC and iron metabolism proteins was assessed in SW480 cells (a cell line with deregulated Wnt signaling) before and after restoration of APC (Figures 1C and 1D). We saw that challenging SW480 cells with iron further deregulated Wnt signaling targets such as c-MYC (mean 2.7-fold, $p = 0.0004$) and increased the expression of TfR1 (mean 2.7-fold, $p < 0.0001$) and DMT1 (mean 2.3-fold, $p < 0.0001$; Figure 1C). Functionally, this was associated with a 10-fold increase in cellular iron deposition ($p < 0.0001$; Figure 1D). When APC was reconstituted, TfR1 ($p = 0.002$) and DMT1 ($p = 0.003$) were dramatically reduced by more than half following iron treatment (Figure 1C). In addition, the cellular iron levels in SW480 cells with reconstituted APC (control+APC) were statistically decreased to one-fifth relative to sham transfected cells ($p = 0.0053$) and also moderately decreased when cultured in the presence of high iron (iron versus iron+APC, $p = 0.0048$; Figure 1D). As previously reported (Brookes et al., 2008), the iron-mediated induction of cellular proliferation was no longer observed when WT APC was reconstituted into these cells.

Association of Wnt Signaling with TfR1, DMT1, and Ferritin Expression

To further support the relationship between deregulated Wnt signaling and the expression TfR1, DMT1, and ferritin, we assessed the expression of *c-Myc* (a key target of canonical Wnt signaling), *TfR1*, *DMT1*, and *ferritin* in $Apc^{Min/+}$ mouse polyps ($n = 8$), human polyps ($n = 20$), and human colorectal carcinomas ($n = 10$), each matched with an adjacent nondiseased control mucosa (Figure 1E). The $Apc^{Min/+}$ mouse model carries a germline mutation in the *Apc* gene and mimics familial adenomatous polyposis, a hereditary form of CRC (Su et al., 1992). The mice develop multiple adenomas and hence represent an early stage of CRC. In all eight $Apc^{Min/+}$ adenomas examined, we observed a marked induction of *c-Myc* mRNA (8/8 mean fold induction of 4.58), *TfR1* (7/8 mean fold increase of 2.6) and *DMT1* mRNA (7/8 mean fold increase of 3.2) compared with nondiseased adjacent tissue. A statistical analysis suggested a robust correlation of *c-Myc* with *TfR1* ($p < 0.004$) and *DMT1* ($p < 0.001$) expression; however, no relationship was observed with *ferritin*, which was overexpressed in five of the eight samples. Furthermore, this induction of *c-Myc*, *TfR1*, and *DMT1* was also observed in human adenomas (16/20, 16/20, and 15/20, respectively) and carcinomas (10/10, 7/10, and 9/10, respectively). *Ferritin* mRNA was overexpressed in only 10/20 and 4/10 human adenomas and carcinomas, respectively.

Because previous studies have shown that c-MYC may regulate the expression of TfR1 by directly binding to its promoter region, as well as by indirectly regulating the iron regulatory protein 2 (IRP2) and ferritin, we overexpressed c-MYC in the RKO cell line using the well-characterized *c-MycER* system (Figure 2; Littlewood et al., 1995; O'Donnell et al., 2006; Wu et al., 1999). c-MYC induction mediated by tamoxifen treatment resulted in increased mRNA of *TfR1* (mean 2.1-fold, $p = 0.017$) and *DMT1* (mean 1.9-fold, $p = 0.0005$), whereas ferritin protein expression was repressed compared with non-tamoxifen-treated cells ($p < 0.0001$; Figures 2A–2D). Upon *c-MYC* activation in the presence of iron, an almost double cellular iron acquisition was observed compared with non-tamoxifen-treated cells challenged with iron (Figure 2E). To further confirm a direct regulation of these proteins by c-MYC, we deleted c-MYC in the adult murine intestine. To that end, we generated $AHCre^{+}$ $c\text{-}Myc^{fl/fl}$ mice. The AH Cre transgene yields highly penetrant Cre expression in the intestine following injection of beta-naphthoflavone and thus allows *c-Myc* to be inducibly deleted from the adult intestine (de Alboran et al., 2001; Sansom et al., 2007). Our previous studies showed that short-term deletion of c-MYC does not affect intestinal homeostasis, and that Wnt gene activation and the phenotypes of APC loss are dependent on c-MYC activity (Sansom et al., 2004, 2007). While investigating mRNA levels in vivo in WT versus *c-Myc* deleted intestines, we noted a significant downregulation of *DMT1* by almost half ($p = 0.0018$) upon *c-Myc* loss. In contrast, TfR1 was not affected upon *c-Myc* deletion alone, but was significantly decreased to almost one-third in mice that had a combined deficiency for APC and c-MYC when compared with APC-deficient intestines alone ($AHCre^{+}$ $Apc^{fl/fl}$ $c\text{-}MYC^{fl/fl}$ versus $AHCre^{+}$ $Apc^{fl/fl}$, $p = 0.02$). Therefore, in vivo c-MYC levels are important for the expression of components of the iron import machinery.

Iron Modifies Intestinal Tumorigenesis

Given these clear mechanistic links between Wnt signaling and cellular iron protein machinery, and the upregulation of these proteins in the very early stages of CRC carcinogenesis, we next examined whether modifying the levels of iron could affect intestinal tumorigenesis in vivo. To that end, we examined whether a diet completely lacking iron [the iron-deficient diet (IDD)] could suppress tumorigenesis, and a diet with excess iron [the carbonyl iron diet (CID)] could stimulate tumorigenesis in the $Apc^{Min/+}$ mouse (Su et al., 1992). In this mouse model, loss of the remaining WT *Apc* allele initiates tumorigenesis early in life and the mice develop hundreds of adenomas throughout their small intestine and colon by 100 days of age. $Apc^{Min/+}$ mice were fed either an IDD ($n = 16$) or a control diet (CD; $n = 17$) from weaning and were euthanized at 80 days of age (Figures 3A–3C). We determined the tumor burden by assessing tumor number and size from whole-mount intestines. $Apc^{Min/+}$ mice fed the IDD developed a greatly reduced tumor burden

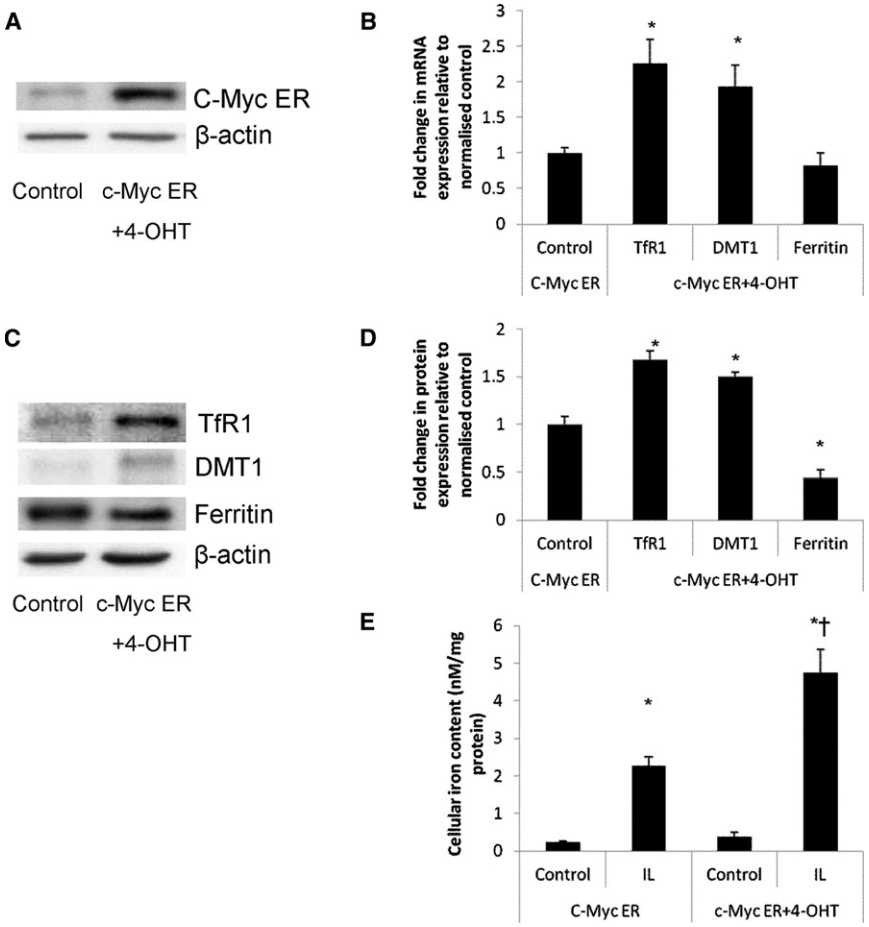

Figure 2. Effect of c-Myc Overexpression on Cellular Iron Metabolism

RKO cells were transiently transfected with either pCDNA3.1/Zeo-MYCER or empty vector, and the chimeric protein was then activated by the addition of 4-OHT.

(A) Representative western blot demonstrating the expression of the chimeric protein.

(B) c-MYC overexpression resulted in increased *TfR1* and *DMT1* mRNA expression ($p = 0.017$ TfR1, $p = 0.0005$ DMT1, Student's t test). Data are presented as mean ± SEM.

(C) Representative western blot indicating expression levels of TfR1, DMT1, and ferritin in control and c-MYC overexpressing cells. B-actin was employed for protein normalization.

(D) c-MYC overexpression resulted in increased TfR1 and DMT1, and decreased ferritin protein expression ($p = 0.0025$ TfR1, $p = 0.046$ DMT1, $p < 0.0001$ ferritin, Student's t test). Data are presented as mean ± SEM.

(E) To assess the influence of activated c-MYC ER on cellular iron (IL) levels, cells were cultured in the presence and absence of 4-OHT and IL. Activated c-MYC ER and IL (c-Myc ER+4-OHT+IL) enhanced cellular IL loading compared with cells with no IL (c-Myc ER+4-OHT) and in nonactivated c-MYC ER cells challenged with IL (c-Myc ER+IL; $p < 0.0001$ c-Myc ER+4-OHT+IL versus c-Myc ER+4-OHT, $p = 0.0016$ c-Myc ER+4-OHT+IL versus c-Myc ER+IL, Student's t test). Data are presented as mean ± SEM; * denotes statistical significance compared with control; † denotes statistical significance compared with c-Myc ER+IL.

by more than half ($p < 0.0001$), with a marked reduction in both tumor number ($p < 0.0001$) and size ($p = 0.0006$). WT mice treated with the IDD remained healthy and showed no intestinal phenotypes within the time course of the experiment. Furthermore, $Apc^{Min/+}$ mice on the IDD were healthy and gained weight at the same rates as controls (Figure S1). In contrast, mice fed an iron-rich diet (CID; 2% carbonyl iron w/w; n = 13) rapidly began to show signs of intestinal neoplasia and thus had to be harvested at 60 days of age (Figures 3D and 3E). Due to the rapid development of intestinal tumorigenesis and the resulting ill health of the mice, we assessed tumor burden by scoring tissue sections for the number of tumors present within the first 10 cm of the small intestine. The CID resulted in a 2- to 3-fold amplification in tumorigenesis compared with mice on the CD sacrificed at the same 60-day time point ($p = 0.002$; Figure 3D). Overall, the 2% carbonyl iron resulted in higher levels of iron in both normal intestine and adenomas compared with the CD, as detected by Perls' Prussian staining (Figure 3F; Figure S2). Of importance, previous reports indicate that in the short term, this level of dietary iron overload is not enough to cause liver toxicity, which suggests that the ill heath was due to the formation of multiple intestinal adenomas (Pigeon et al., 1999).

Given that tumor formation in the $Apc^{Min/+}$ mice occurred following loss of the remaining *Apc* allele, it is possible that iron affects both tumor growth and initiation by increasing the mutation rates of the WT allele. Therefore, we next assessed whether the IDD and CID could modify tumorigenesis following the loss of both copies of *Apc*. For these studies we used the $Lgr5creERT2^{+}$ $Apc^{fl/fl}$ model, which has *Apc* deletion solely in stem cells (Barker et al., 2007). This represents a rapid model of intestinal tumorigenesis, with mice developing numerous adenomas within 50 days following Cre induction. $Lgr5creERT2^{+}$ $Apc^{fl/fl}$ mice were placed on IDD (n = 18), CID (n = 17), or CD (n = 24), and following a 2-week dietary acclimatization were treated with tamoxifen to induce Cre-mediated recombination of *Apc* and allowed to age until signs of ill health were observed (Figure 4A). In this potent model of intestinal tumorigenesis, IDD strongly attenuated tumorigenesis, as indicated by the extended survival of mice on the IDD compared with the CD (median survival 89 days (IDD) versus 61 days (CD), $p = 0.001$, Kaplan Meier method, logrank). Again, the IDD did not have any adverse effects on the health of the mice as assessed by weight monitoring (Figure S3). Conversely, mice on the CID had a dramatically shortened survival period compared with mice on the CD (median survival 42 days (CID) versus 61 days (CD), $p = 0.001$, Kaplan Meier method, logrank).

To confirm that the cause of ill health in the CID group was due to increased tumorigenesis, we next performed a time-point experiment soon after Cre induction. For this experiment we again used the $Lgr5creERT2^{+}$ $Apc^{fl/fl}$ mice, but this time

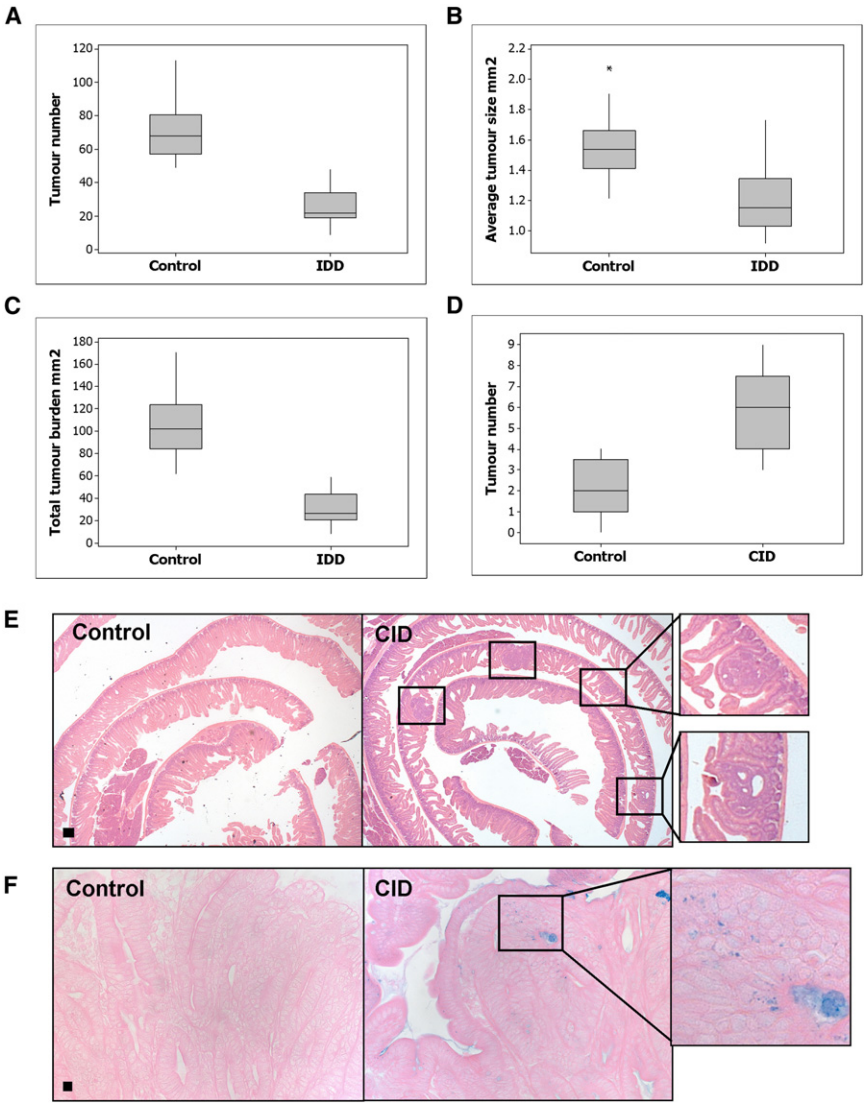

Figure 3. Iron Modifies Intestinal Tumorigenesis in the *Apc*$^{MIN/+}$ Mouse

(A–C) Tumor number, size, and burden comparison between CD- and IDD-fed mice at 80 days of age ($p < 0.0001$ number, burden, $p = 0.0006$ size, Mann-Whitney).

(D) Tumor number comparison on section (first 10 cm of intestine) between CD- and CID-fed mice at 60 days of age ($p = 0.002$, Mann-Whitney).

(E) Representative H&E pictures of intestines from CD- and CID-fed mice. Panels highlight numerous small adenomas in the CID-fed mice. Scale bar: 200 μm.

(F) Perls' Prussian blue staining of adenomas from control and CID-fed mice showing iron deposits within the CID tumors. Scale bar: 10 μm. See also Figures S1 and S2.

administered a higher induction regime (four injections of tamoxifen over 4 days) to obtain more incipient adenomas, and took them at an early time point (day 15 post induction). At this stage, the mice on the CD (n = 3) had small lesions in the intestine visible on section but were otherwise without a phenotype. In contrast, the mice on the CID (n = 3) were already displaying signs of ill health at the same time point (day 15) and upon harvesting, they presented a thickened intestine, a hallmark of multiple adenomas. Figures 4B–4D show that the CID led to a drastic increase in both number and size at this early time point ($p = 0.04$). These lesions also show marked iron deposits in enterocytes, as detected by Perls' Prussian staining, in contrast to CD lesions, in which such deposits are absent (Figure S3).

The *Lgr5creERT2*$^{+}$ construct contains a green fluorescent protein (GFP) reporter knocked into the endogenous leucine-rich repeat containing a G protein-coupled receptor 5 (*Lgr5*) locus, which allows visualization of cells that express Lgr5 (Barker et al., 2007). Elegant studies by Merlos-Suárez et al. (2011) and van der Flier et al. (2007, 2009) showed that Lgr5 marks a stem cell population in the normal intestine that is retained within adenomas, and this may reflect a cancer stem cell population. A detailed characterization of the Lgr5-GFP population showed that this marks a particular subset of Wnt target genes that define the stem cell population. Therefore, examination of GFP expression may allow assessment of the Wnt stem cell gene expression, which is pertinent given our previous in vitro studies linking iron to activating Wnt signaling (de Lau et al., 2011). When we examined whole-mount intestines for the levels of GFP expression in the *Lgr5creERT2*$^{+}$ *Apc*$^{fl/fl}$ mice on the CID, we noticed a marked increase compared with mice on the CD (Figure 4E). To assess whether this was specific to intestinal cells with modifications in the Wnt pathway, we crossed the *Apc*$^{Min/+}$ mice with *Lgr5creERT2*$^{+}$ mice. By using the GFP reporter in these mice, we were able to assess Lgr5 expression using multiphoton microscopy to create a 3D reconstruction of the intestinal crypts. In the normal epithelium, cells positive for GFP expression (and hence Lgr5 expression) are located at the bottom of the crypt. Of importance, we found a significant 1.5- to 2-fold increase in the area occupied by Lgr5-positive intestinal stem cells in mice carrying the *Apc*$^{Min/+}$ allele (Figure 4F; Figure S4). This was in contrast to *Lgr5creERT2*$^{+}$ *Apc*$^{+/+}$ mice on the CID, which had the same volume of Lgr5 intestinal stem cells as mice on the CD. This demonstrates once more that iron sensitivity is strictly related to *Apc* status both in vivo and in vitro.

Iron Levels Govern the Cellular Fate of *Apc*-Deficient Cells

After determining that iron levels were potently modifying tumorigenesis, we next wanted to investigate the direct impact

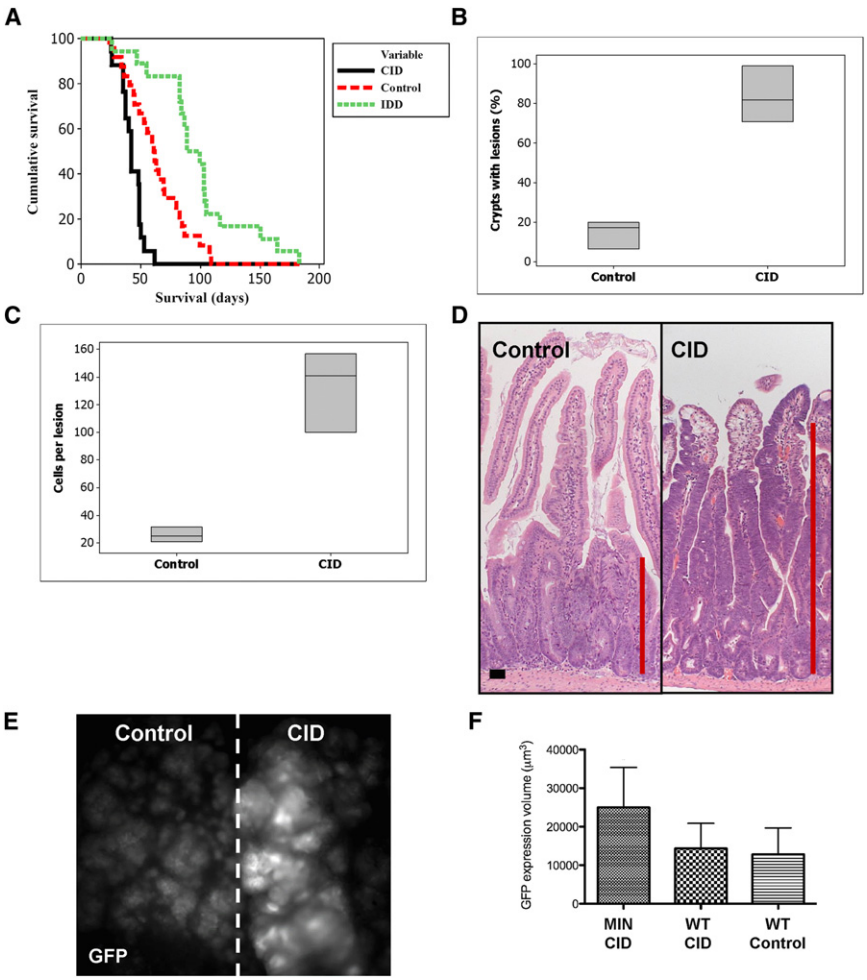

Figure 4. High Iron Drives Intestinal Tumorigenesis and Lgr5 Expression

(A) Kaplan-Meier survival plot for *Lgr5creERT2*$^{+}$ *Apc*$^{fl/fl}$ mice on IDD, CD, or CID (p = 0.001, logrank, IDD versus CD, and CID versus CD).

(B) Percentage of crypts with lesions (in intestines from *Lgr5creERT2*$^{+}$ *Apc*$^{fl/fl}$ mice on CD or CID at day 15 post-induction. A lesion was defined as a clump of >10 cells with nuclear β-catenin accumulation. Each individual crypt (from a strip of 10 cm of intestine) was assessed for the presence or absence of a lesion (p = 0.04, Mann-Whitney).

(C) The average number of cells displaying nuclear β-catenin per lesion (as a measure of size) in intestines from *Lgr5creERT2*$^{+}$ *Apc*$^{fl/fl}$ mice on control or CID at day 15 post-induction (p = 0.04, Mann-Whitney).

(D) Representative H&E pictures of intestines from *Lgr5creERT2*$^{+}$ *Apc*$^{fl/fl}$ CD- and CID-fed mice at day 15 post-induction. Red lines highlight the size of the Apc-deficient crypts. Scale bar: 10 μm.

(E) In vivo GFP fluorescence imaging of whole-mount intestines from *Lgr5creERT2*$^{+}$ *Apc*$^{fl/fl}$ mice on CD or CID (end of tumorigenesis). Tumors express GFP.

(F) Measurement of Lgr5 cell volume, via the GFP label, in vivo in normal crypts using a multiphoton laser microscope. MIN CID: *Lgr5creERT2*$^{+}$ *Apc*$^{MIN/+}$ on high iron for 2 weeks. WT CID: *Lgr5creERT2*$^{+}$ *Apc*$^{+/+}$ littermate on high iron for 2 weeks. WT control: *Lgr5creERT2*$^{+}$ *Apc*$^{+/+}$ on CD (age matched). A minimum of 60 crypts were measured per mouse (MIN CID versus WT CID, p < 0.0001, Mann-Whitney). Error bars represent standard deviation (SD).

See also Figures S3 and S4.

of iron on intestinal enterocytes that have acutely lost both copies of the *Apc* gene. To that end, we generated *AHCre*$^{+}$ *Apc*$^{fl/fl}$ mice and studied the impact of iron modulation 4 days after *Apc* gene deletion (Sansom et al., 2004). Mice were placed on the IDD (n = 5), CID (n = 3), or CD (n = 5) for 2 weeks before induction. Figures 5A–5C show that the CID increased proliferation rates by 4- to 5-fold following *Apc* loss (p = 0.015), whereas the IDD promoted a marked increase in apoptosis by 2- to 3-fold (p = 0.015). This is in good agreement with the tumor burden outcomes obtained earlier in *Apc*$^{Min/+}$ mice for the two diets, i.e., an increase in apoptosis gave rise to slow-growing, small tumors in mice on the IDD, whereas an increase in proliferation resulted in larger, more aggressive tumors in mice on the CID. We also looked at the effect of both diets on WT intestines (Figure S5), and we noted no change in the mitotic or apoptotic index for animals on the CID, but an increase in both mitosis and apoptosis in mice on the IDD. However, this increase in both apoptosis and mitosis did not alter the crypt size (compared with CD), indicating that WT intestines are able to cope with the lack of iron by maintaining a careful balance between proliferation and death. We also carefully monitored the health and potential anemia of the mice on the IDD by weighing the mice and obtaining blood cell counts at the end of the experiment (Figures S5 and S6).

We then scored apoptosis and mitosis in the tumors from *Lgr5creERT2*$^{+}$ *Apc*$^{fl/fl}$ survival cohorts to see if these effects on proliferation and apoptosis were retained throughout tumorigenesis. Figures 5D–5F show that adenomas from the iron-deficient mice still retained a higher level of apoptosis (p = 0.006), and the tumors that developed on the CID had overall more proliferation (p = 0.006). Thus, the levels of iron directly affect the ability of *Apc*-deficient cells to survive and proliferate both immediately following *Apc* loss and within adenomas.

To confirm our in vitro results showing that *Apc*-deficient cells had high levels of TfR1 and DMT1 in vivo, and that these were not downregulated following iron administration, we examined the mRNA levels by quantitative reverse transcriptase (qRT)-PCR. In order to isolate a purer intestinal cell population, we used the laser capture microdissection (LCM) technique, which enabled us to microdissect specific parts of the intestinal crypt villus structure and thus enrich in the epithelial cells of choice (Potter and Brunskill, 2012). We found that mice on the CID had dramatically increased levels of *TfR1*, *DMT1*, and *ferritin* following *Apc* gene deletion compared with WT mice on the same diet (Figure S7). Moreover, to further examine whether there was an additional expansion of the intestinal stem cell (ISC) signature following Apc loss, we looked specifically at the

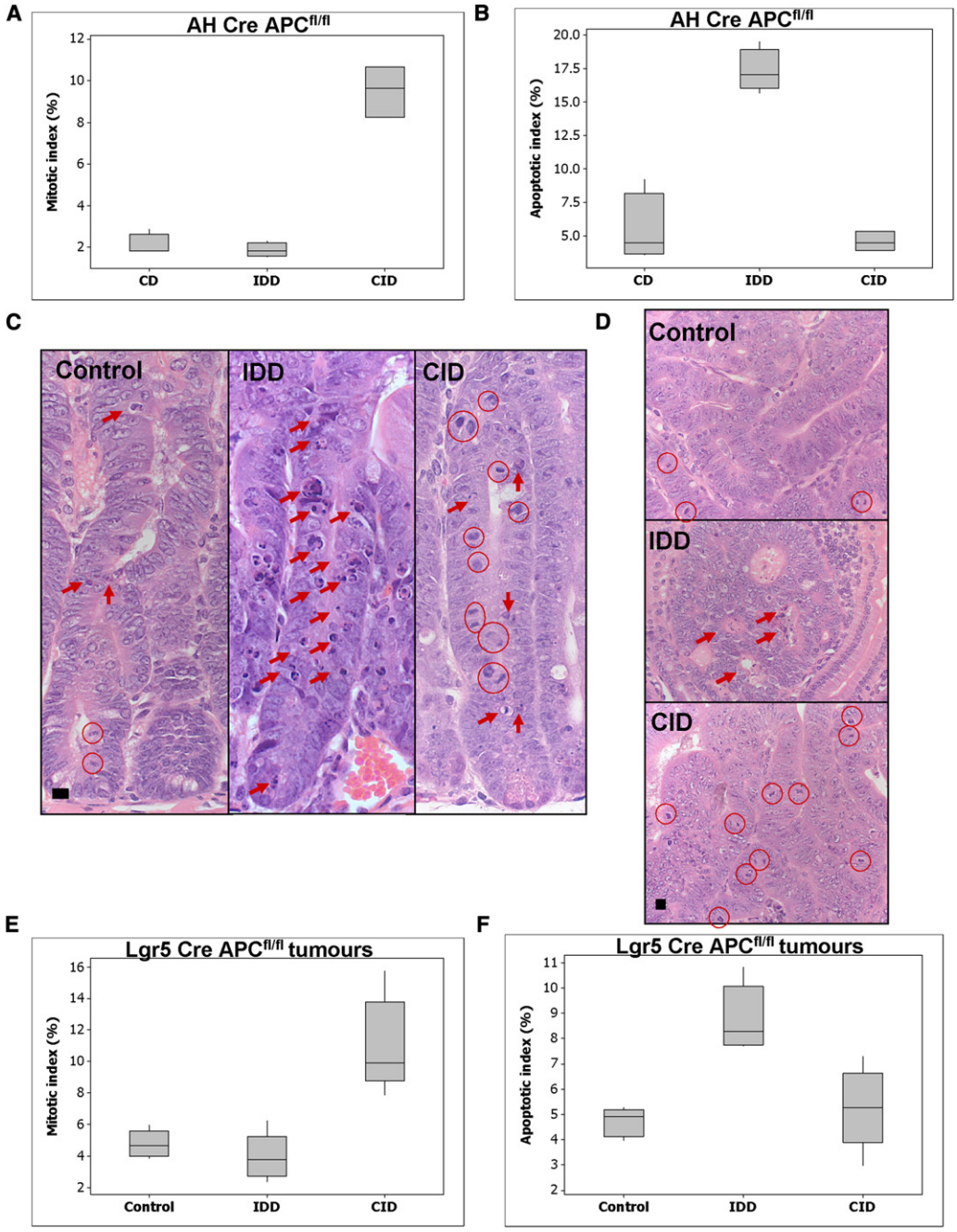

Figure 5. Iron Levels Modulate Proliferation and Apoptosis Immediately after Apc Loss In Vivo

(A) Mitotic index as percentage of cells in mitosis per crypt in *Apc*-deficient enterocytes from *AHCre*$^{+}$ *Apc* $^{fl/fl}$ mice on CD, IDD, or CID at day 4 post-induction ($p = 0.015$, CID versus CD, and CID versus IDD, Mann-Whitney).

(B) Apoptotic index as percentage of cells in apoptosis per crypt in *Apc*-deficient enterocytes from *AHCre*$^{+}$ *Apc* $^{fl/fl}$ mice on CD, IDD, or CID at day 4 post-induction ($p = 0.015$, IDD versus CD, and IDD versus CID, Mann-Whitney).

(C) Representative H&E pictures of intestines from *AHCre*$^{+}$ *Apc*$^{fl/fl}$ mice on CD, IDD, or CID at day 4 post-induction. Arrows indicate apoptotic bodies. Circles indicate mitotic figures. Scale bar: 10 μm.

(D) Representative H&E pictures of adenomas from *Lgr5creERT2*$^{+}$ *Apc*$^{fl/fl}$ mice on CD, IDD, or CID at endpoint tumorigenesis. Arrows indicate apoptotic bodies. Circles indicate mitotic figures. Scale bar: 10 μm.

(E) Mitotic index as percentage of cells in mitosis per adenoma in *Lgr5creERT2*$^{+}$ *Apc*$^{fl/fl}$ mice on CD, IDD, or CID at endpoint tumorigenesis ($p = 0.006$, CID versus CD, and CID versus IDD, Mann-Whitney).

(F) Apoptotic index as percentage of cells in apoptosis per adenoma in *Lgr5creERT2*$^{+}$ *Apc*$^{fl/fl}$ mice on CD, IDD, or CID at endpoint tumorigenesis ($p = 0.006$, IDD versus CD, and IDD versus CID, Mann-Whitney). See also Figures S5 and S6.

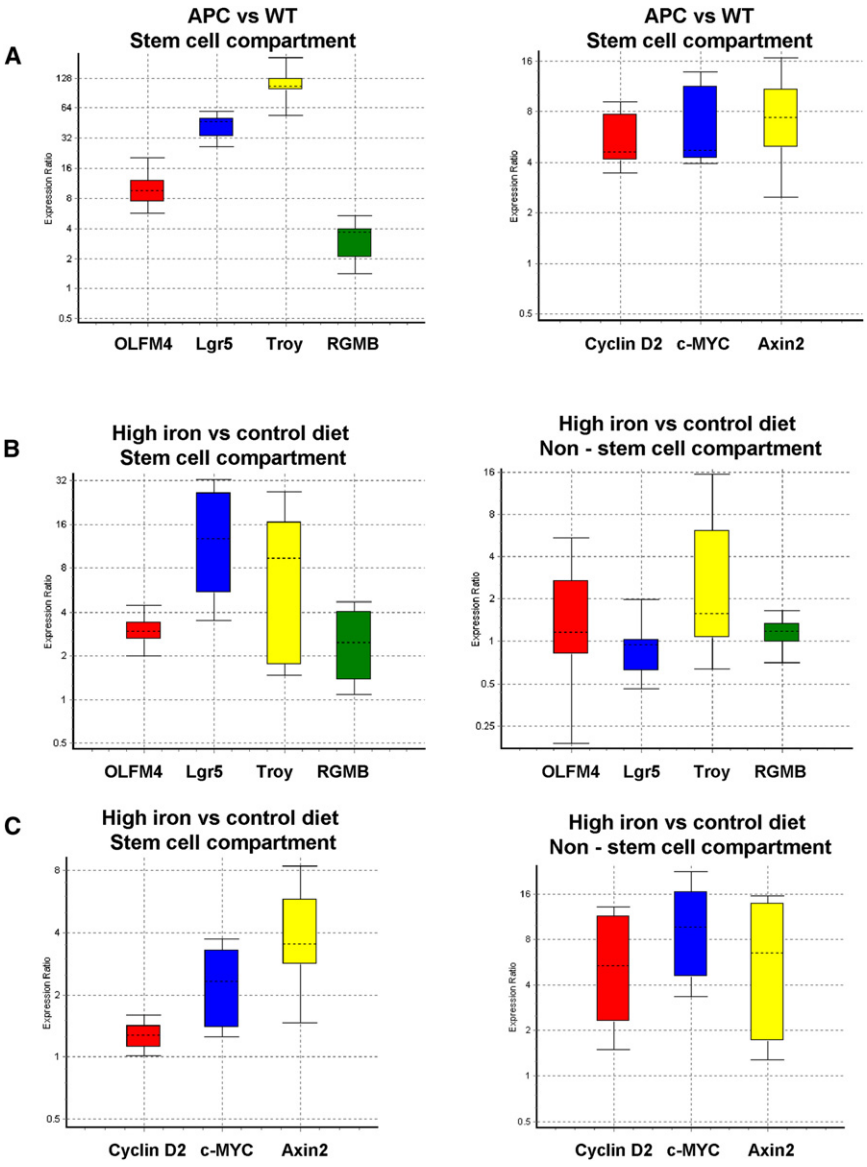

Figure 6. High Iron Levels Alter Stem Cell Gene Expression following Apc Loss In Vivo

A population of cells highly enriched in intestinal stem cells was obtained by LCM of the bottom half of the intestinal crypt in WT and *Apc*-deficient mice (day 4 post-induction). A second population of cells was isolated away from the stem cell zone but still within the recombined area of the crypt and villus, representing the non-stem-cell zone. qRT-PCR analysis of the expression of a panel of stem cell and Wnt target genes was performed in these stem-cell-enriched and non-stem-cell-zone populations.

(A) mRNA levels of stem cell genes *Olfm4*, *Lgr5*, *Troy*, and *Rgmb* (left panel), as well as Wnt target genes *Cyclin D2*, *c-Myc*, and *Axin2* (right panel), are all increased following *Apc* loss in mice on the CID compared with WT mice on the same diet ($p < 0.01$).

(B) mRNA levels of stem cell genes *Olfm4*, *Lgr5*, *Troy*, and *Rgmb* are increased in the stem cell compartment of *Apc*-deficient mice on the CID compared with CD (left panel, $p < 0.01$). There is no difference in the expression of these stem cell genes in the non-stem cell compartment between diets.

(C) mRNA levels of Wnt target genes *Cyclin D2*, *c-Myc*, and *Axin2* are increased in both the stem cell compartment (left panel) and the non-stem cell compartment (right panel) of *Apc*-deficient mice on the CID compared with CD ($p < 0.01$). See also Figure S7.

stem cell compartment (bottom of the crypt) for the expression levels of the ISC signature genes olfactomedin 4 (*Olmf4*), *Lgr5*, tumor necrosis factor receptor superfamily member 19 (*Troy*) and RGM domain family member B (*Rgmb*; van der Flier et al., 2009). These genes were all significantly upregulated in *Apc*-deficient mice treated with high iron compared with WT mice on the same diet (Figure 6A). To verify that this was not simply a reflection of an increased ISC signature following Wnt activation (via *Apc* loss), we compared the expression in CID versus CD within the same stem/progenitor cell zone. Our results show that there was a significant increase in the ISC targets in the iron-treated mice. This was specific to the crypt base, as LCM of the top of the crypt did not show an increase in stem cell genes even though these cells are also *Apc*-deficient (Figure 6B). However, Wnt target genes such as *c-Myc*, *Axin2*, and *Cyclin D2* were upregulated in both the crypt base and the top of the crypt in the CID group, which is consistent with Wnt pathway activation throughout the crypt and villus (Figure 6C).

Delineating the Pool of Iron that Is Responsible for Rescuing Tumorigenesis

Although our data clearly demonstrate a role for iron in tumorigenesis, they fail to delineate the pool of iron, as one would expect that feeding an IDD would result in decreased luminal iron levels and also chronically mediate a systemic iron deficiency. Thus, in an attempt to separate these two pools of iron, $Apc^{Min/+}$ mice were fed an IDD but maintained systemically iron replete (IDD+IDex) by subcutaneous injections of iron dextran (IDex; Theurl et al., 2005). Briefly, $Apc^{Min/+}$ mice were put on the IDD at weaning and given two subcutaneous injections of 50 mg IDex on two consecutive days to reach systemic iron overload. The iron load status was maintained with an additional subcutaneous injection of 50 mg IDex each month. The results of these studies again demonstrate a suppressed tumor burden compared with mice on the CD ($p = 0.004$; Figures 7A–7C). Furthermore, Perls' Prussian blue staining of the intestines from IDD+IDex-treated mice does not show intestinal iron deposits, in contrast to mice on the CID, highlighting the fact that systemic iron overload does not lead to iron accumulation

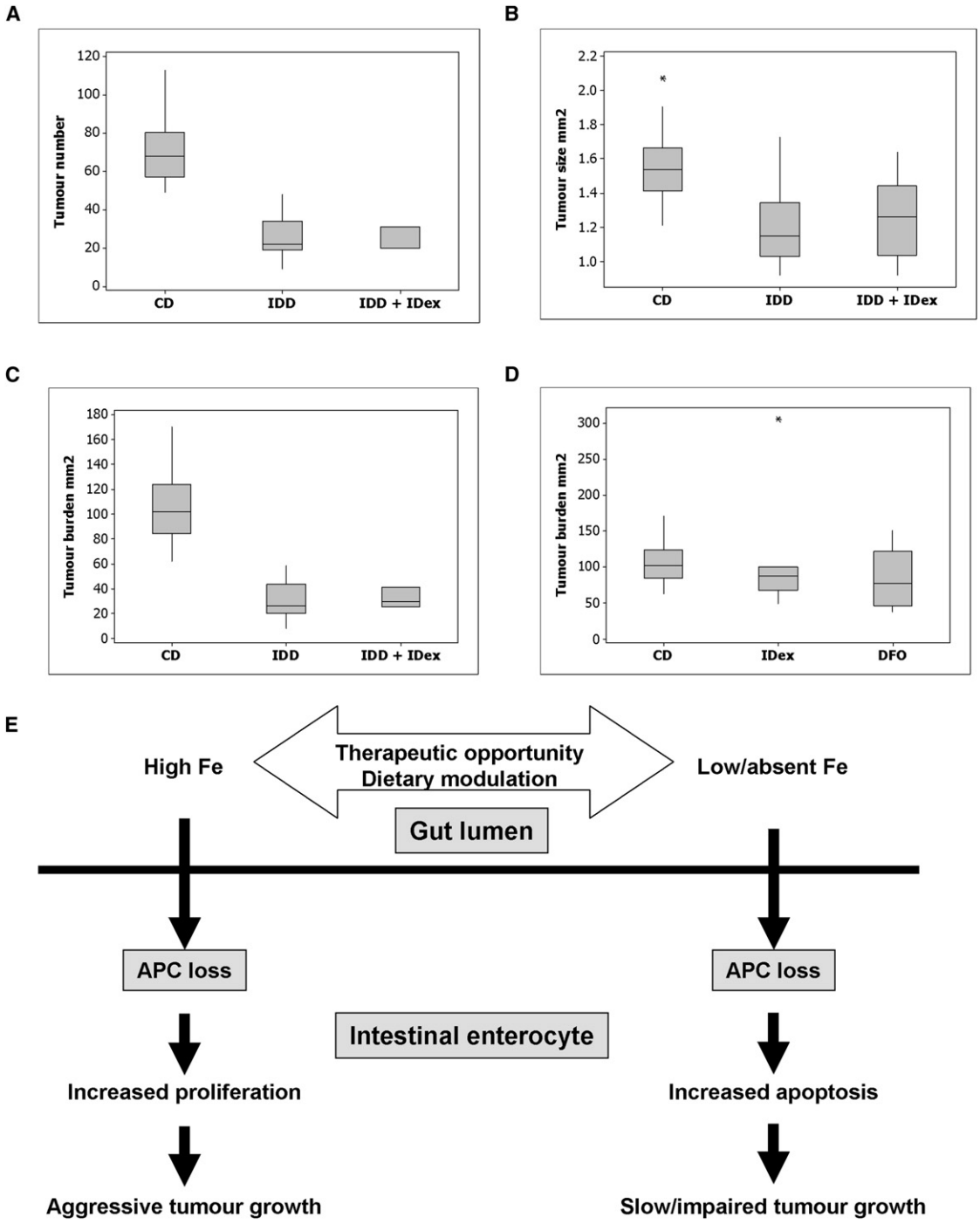

Figure 7. The Luminal Iron Pool Is Responsible for Intestinal Tumor Formation In Vivo

(A–C) Tumor number, size, and burden comparison between CD, IDD, and IDD+IDex treatment (IDD+IDex) *Apc*$^{MIN/+}$ mice at 80 days of age. Systemic iron overload via IDex treatment does not affect the tumor protection conferred by the lack of dietary iron.

(D) Tumor burden comparison between *Apc*$^{MIN/+}$ mice with systemic iron overload (IDex), systemic iron chelation (DFO), or CD alone (CD).

(E) Overview representing the therapeutic opportunity offered by dietary iron modulation.

in intestinal tissue (Figure S2). However, these observations do not rule out the possibility that the systemic injections of IDex could have had an impact on tumorigenesis, so we further treated a separate cohort of *Apc*$^{Min/+}$ mice (n = 9), this time on a CD, and administered IDex as before. We failed to observe any influence on tumor burden at 80 days (Figure 7D).

Furthermore, decreasing the level of systemic iron in $Apc^{Min/+}$ mice (n = 8) by administering daily injections of a potent iron chelator, desferrioxamine (DFO), also failed to affect tumorigenesis. Taken together, these data suggest that the systemic iron pool has little effect on intestinal tumorigenesis, but luminal iron is crucial.

DISCUSSION

In this study, we show that spontaneous intestinal neoplasia driven by the loss of the key intestinal tumor suppressor *Apc* is highly dependent on iron. Moreover, we demonstrate that an excess of iron promotes intestinal tumorigenesis, and that tumorigenesis was markedly suppressed in mice fed an IDD. Our observations provide an explanation for previous results from human epidemiological studies that point to high dietary iron intake as a risk factor for tumorigenesis (Kato et al., 1999; Lee et al., 2004; Mainous et al., 2005; Nelson, 2001; Nelson et al., 1995; Shaheen et al., 2003; Weinberg, 1994). In addition to demonstrating that iron excess drives tumorigenesis in the background of an aberration in *Apc*, we also identified the luminal iron pool (rather than the circulating iron pool) as the major driver of carcinogenesis.

One of the most exciting findings from our studies is that *Apc*-deficient cells appear to require precise levels of iron for efficient tumorigenesis in vivo. Removal of iron drives apoptosis of *Apc*-deficient cells, and raising the levels of iron increases proliferation, which suggests that levels of iron are critical for the cellular fate following *Apc* loss. By altering the outcome of an *Apc* mutation, one would predict that this could account for changes in the lifetime risk of iron exposure. Of importance, our studies investigating the impact of iron on WT intestinal enterocytes showed that even very high levels of iron did not lead to spontaneous tumorigenesis. Therefore, it is the impact of iron on cells that have deregulated Wnt signaling that is crucial. This is consistent with our in vitro data showing that downregulation of Wnt signaling (through APC addition) alters the proliferation of CRC cell lines, and our in vivo data showing deregulation of iron import proteins at the early stages of adenoma formation in both humans and mice. In support of the importance of a link among Wnt signaling, iron, and colorectal neoplasia, a recent study showed that a class of iron chelators, acyl hydrazones, abrogate Wnt signaling and growth of CRC cell lines with constitutive Wnt signaling (Song et al., 2011).

In the context of human CRC, one issue that has been difficult to resolve is the particular genotype–phenotype relationship of the sporadic *Apc* mutations that occur. Rather than a complete loss-of-function mutation in the *Apc* gene, specific mutations leading to a truncated protein that can bind β-catenin but not Axin may occur. These mutant proteins still cannot turn over β-catenin, but may still be able to more subtly modulate Wnt signaling activity. Knockin of the common human mutation Apc^{1322T} in the mouse leads to faster tumorigenesis than the $Apc^{Min/+}$ mutation (Pollard et al., 2009). Wnt target gene activation in the model is modestly altered with a reduction in many Wnt targets but an increase in Lgr5 and other stem cell markers (Lewis et al., 2010). Given the increased levels of Lgr5 we observed in $Apc^{Min/+}$ mice following iron treatment, it is tempting to speculate that one of the mechanisms by which iron may increase the lifetime risk of CRC is to increase the number of stem cells that carry a single *Apc* mutation. These cells could then act as highly efficient cells of origin for intestinal cancer, and hence increase the number of target cells for transformation. Indeed, we found that *Apc* loss combined with a CID upregulated the stem cell signature in the stem cell zone.

However, in addition to iron fueling Wnt signaling and other cellular processes, such as DNA synthesis, iron also likely contributes to increased free-radical-mediated cellular damage (e.g., lipid peroxidation and DNA damage) due to its propensity to be involved in Fenton reaction chemistry (Toyokuni, 1996, 2009). Further studies to elucidate the precise contribution of these factors to CRC initiation and progression will be of great interest. For example, modulation of reactive oxygen species levels was shown to have a considerable impact on intestinal stem cell proliferation in *Drosophila* (Biteau et al., 2008), and antioxidants are associated with protection against CRC.

Taken together, our data provide strong support for the notion that luminal iron cooperates with Apc loss to promote intestinal tumorigenesis, and that chelation of this pool of iron may provide a platform for therapeutic intervention (Figure 7E) in individuals at high risk of developing CRC (e.g., individuals with colorectal adenomas and inflammatory bowel disease). Individuals with these conditions commonly present with systemic anemia, and current practice is to treat such patients with high doses of oral iron. According to our observations, this is likely to both exacerbate their condition and elevate their risk of developing CRC. Instead, we suggest that such patients should be supplemented systemically with intravenous infusions of iron and concurrently receive colonic luminal iron chelation therapy. Such a protocol would resolve the anemia and at the same time diminish the carcinogenic pool of iron residing with the colon.

EXPERIMENTAL PROCEDURES

Ethics Statement

All mouse experiments were performed according to the UK Home Office guidelines. The research was approved by the Glasgow University Ethics Committee. Work with human samples was carried out in accordance with the Declaration of Helsinki (2000) of the World Medical Association. This study was approved by the ethics committee of the Birmingham and Black Country Comprehensive Local Research Network (LREC no. 10/H1202/40). All patients provided informed written consent. Samples (n = 10) of colorectal carcinoma and colorectal polyps (n = 20), each matched with normal colonic mucosa, were collected during either endoscopy or surgery, and each tissue specimen was processed into mRNA and subjected to qRT-PCR.

Mouse Colonies

Outbred mice segregating for the C57BL6J and S129 genomes (five generations C57Bl6J) were used from 4 to 8 weeks of age. The following alleles were used: *AH Cre* (Ireland et al., 2004), *Lgr5-EGFP-IREScreERT2* (Barker et al., 2007), Apc^{MIN} (Su et al., 1992), Apc^{580Sfl} (Shibata et al., 1997), and $c\text{-}MYC^{fl}$ (de Alboran et al., 2001). Only male mice were used in this study.

Iron Modulation

For luminal iron modulation, three diets were purchased from Harlan Laboratories UK: TD 80396 (IDD), TD 80394 (48 ppm added iron; CD), and TD 08496

(CID). Male $Apc^{MIN/+}$ and WT littermates were placed on the respective diet at weaning (~30 days of age) and were aged to a time point of 80 days of age. Mice on the CID were taken due to illness at 60 days of age. To ensure that the diets had no adverse effects, three WT mice from each group were kept on each diet for 3 months. For systemic iron modulation, male $Apc^{MIN/+}$ and WT littermates were injected with IDex (CosmoFer 50 mg/ml; Pharmacosmos, Holbaek, Denmark) or DFO (desferrioxamine mesilate 500 mg; Mayne Pharma, Warwickshire, UK) from weaning up to 80 days of age. IDex was administered subcutaneously (subcut) at 50 mg per dose on 2 consecutive days at the start of the treatment and once a month subsequently to keep the systemic iron levels high. DFO 200 mg/kg was injected intraperitoneally (i.p.) daily for the duration of the treatment to ensure effective systemic iron chelation. A combined IDD and IDex treatment was also administered from weaning, with mice receiving their first IDex injection the day they were put on the IDD. The IDex treatment regime was continued as above while mice were kept on the IDD until the 80 day time point.

Gene Deletion In Vivo

Adult male mice (6–8 weeks of age) were put on the IDD or CID for 2 weeks before gene manipulation to ensure diet acclimatization. For the survival study, $Lgr5creERT2^{+}$ $Apc^{fl/fl}$ mice on IDD, CD, or CID were injected with a single dose of 3 mg tamoxifen (Sigma, Dorset, UK) i.p. and aged until they showed signs of illness. For time-point experiments, $Lgr5creERT2^{+}$ $Apc^{fl/fl}$ mice on the IDD, CD, or CID were injected for 4 consecutive days with 3 mg (day 0), 2 mg (day 1), 2 mg (day 2), and 2 mg (day 3) tamoxifen i.p., and were taken at day 15 post-induction. $AHCre^{+}$ $Apc^{fl/fl}$ mice on IDD, CD, or CID were injected 3 times in 1 day with 80 mg/kg beta naphthoflavone (Sigma) i.p. and taken at day 4 post-induction. $AHCre^{+}$ $Apc^{fl/fl}$, $AHCre^{+}$ $c\text{-}MYC^{fl/fl}$, and $AHCre^{+}$ $Apc^{fl/fl}$ $c\text{-}MYC^{fl/fl}$ mice on the CD were injected 3 times in 1 day with 80 mg/kg beta naphthoflavone i.p. and taken at day 4 post-induction.

Tumor Scoring

When $Apc^{MIN/+}$ mice reached the 80-day time point, they were culled, and the intestine and colon were removed and scored for tumors on whole mount. WT littermates on the respective diets were also assessed for tumors. For the $Apc^{MIN/+}$ mice on CID (taken at 60 days of age), this was not possible due to the small size of the tumors, so instead their tumors were assessed on hematoxylin and eosin (H&E)-stained sections. The tumors were counted in the first 10 cm of intestine near the stomach. As controls, a separate cohort of $Apc^{MIN/+}$ mice on CD was culled at the same time point of 60 days and assessed for tumors in the same manner. For the $Lgr5creERT2^{+}$ $Apc^{fl/fl}$ mice day 15 experiments, lesions were scored off sections stained for β-catenin (anti-β-catenin mouse monoclonal, 1:50; Transduction Labs, Oxford, UK). A strip of 10 cm of intestine taken from the same position was scored for each mouse (three versus three mice). A lesion was considered as ≥10 cells clumped together and displaying nuclear β-catenin. This was done to distinguish lesions from individual cells positive for nuclear β-catenin found at the bottom of the crypt. To measure the size of the lesions, the total number of nuclear β-catenin-positive cells was counted.

Assaying Apoptosis and Mitosis

The apoptotic and mitotic indexes were scored from H&E sections as previously described (Sansom et al., 2004). For the $AHCre^{+}$ $Apc^{fl/fl}$ day 4 experiments, 25 full crypts were scored from at least three mice of each genotype. For the $Lgr5creERT2^{+}$ $Apc^{fl/fl}$ survival cohorts, five mice were chosen at random for each diet (IDD, CD, and CID) and five tumors were scored per mouse. All of the cells in one tumor were included in the count.

In Vivo Imaging

In vivo imaging of GFP fluorescence within intestinal tissue was performed as follows: intestines were flushed with PBS, opened longitudinally, and imaged using the Olympus OV100 molecular imaging system (Olympus, Southend-on-Sea, UK). In $Lgr5creERT2^{+}$ $Apc^{fl/fl}$ mice, the Lgr5-EGFP-IREScreERT2 construct drives the expression of GFP in cells that express the LGR5 stem cell marker (Barker et al., 2007).

Cell Culture

The human colorectal cell lines SW480 and RKO were selected as examples of lineages containing mutant and WT Apc molecule respectively and were both routinely cultured in Dulbecco's modified eagles medium (GIBCO, USA) with 10% fetal calf serum supplemented with 1% nonessential amino acids, 100 units/ml penicillin and 0.1mg/ml streptomycin. For iron loading experiments cells were challenged upon reaching 70% confluence with either growth medium alone (control) or iron loaded medium (growth medium supplemented with 100 μM $FeSO_4$ and 10 μM sodium ascorbate) for 24 hr and cellular iron loading assessed as previously described (Whitnall et al., 2006).

c-Myc Overexpressing Cell Line

RKO cells were transiently transfected with a c-Myc ER construct (pCNDA3.1-MYCER, a kind gift from Stella Pelengaris, University of Warwick), and 24 hr later some of these cells were treated with 100 nM 4-hydroxytamoxifen (4-OHT) for a further 48 hr. The cells were then lysed and processed into mRNA and protein.

Western Blotting

Western blotting was performed as described previously, with antibodies to c-Myc (C-20, 1:200 dilution; Autogen Bioclear, UK), TfR1 (1:1,000 dilution; Zymed Laboratories), DMT1 (1:1,000 dilution; a kind gift from Prof. G. Anderson, University of Brisbane), ferritin (1:2500 dilution; Sigma), and b-actin (C4, 1:1,000 dilution; Autogen Bioclear, Calne, UK).

Statistics

In Vitro Experiments

Statistical significance was calculated by use of the unpaired Student's t test. All analyses were performed using SPSS version 10.0 (SPSS, Chicago). Significance was accepted at $p < 0.05$. The data presented are the mean of three independent experiments, each performed in triplicate.

In Vivo Experiments

Statistical significance for intestinal tumor scoring (tumor number, size, and burden) was calculated using the nonparametric Mann-Whitney test. For each group, three or more mice were used for comparison. For analysis of survival cohorts, the Kaplan-Meier estimator was used together with the logrank hypothesis test. For all tests, significance was accepted at $p < 0.05$.

Further methods can be found in Extended Experimental Procedures.

SUPPLEMENTAL INFORMATION

Supplemental Information includes Extended Experimental Procedures and seven figures and can be found with this article online at http://dx.doi.org/10.1016/j.celrep.2012.07.003.

LICENSING INFORMATION

ACKNOWLEDGMENTS

We thank Colin Nixon for help with histology, and Derek Miller and Tom Hamilton for help with transgenic work. This work was funded by a Cancer Research-UK Programme Grant to O.S. and a Cancer Research-UK Discovery Committee and Development Grant and Experimental Cancer Medicine Centre funding to C.T. Author contributions: S.R. acquired, analyzed, and interpreted data; performed statistical analysis; and drafted the manuscript. M.J.B. provided samples; acquired, analyzed, and interpreted data; and performed statistical analysis. P.S. acquired, analyzed, and interpreted data. R.A.R. acquired, analyzed, and interpreted data. E.M.G. acquired, analyzed, and interpreted data, and performed statistical analysis. K.A. provided reagents. S.F. acquired and interpreted data. D.S. acquired, analyzed, and interpreted data, and performed statistical analysis. T.I. provided reagents.

C.T. developed the study concept and design, drafted the manuscript, and obtained funding. O.J.S. developed the study concept and design, drafted the manuscript, and obtained funding.

Received: March 1, 2012
Revised: June 1, 2012
Accepted: July 10, 2012
Published online: August 9, 2012

REFERENCES

Barker, N., van Es, J.H., Kuipers, J., Kujala, P., van den Born, M., Cozijnsen, M., Haegebarth, A., Korving, J., Begthel, H., Peters, P.J., and Clevers, H. (2007). Identification of stem cells in small intestine and colon by marker gene Lgr5. Nature *449*, 1003–1007.

Bienz, M., and Clevers, H. (2000). Linking colorectal cancer to Wnt signaling. Cell *103*, 311–320.

Biteau, B., Hochmuth, C.E., and Jasper, H. (2008). JNK activity in somatic stem cells causes loss of tissue homeostasis in the aging *Drosophila* gut. Cell Stem Cell *3*, 442–455.

Brookes, M.J., Hughes, S., Turner, F.E., Reynolds, G., Sharma, N., Ismail, T., Berx, G., McKie, A.T., Hotchin, N., Anderson, G.J., et al. (2006). Modulation of iron transport proteins in human colorectal carcinogenesis. Gut *55*, 1449–1460.

Brookes, M.J., Boult, J., Roberts, K., Cooper, B.T., Hotchin, N.A., Matthews, G., Iqbal, T., and Tselepis, C. (2008). A role for iron in Wnt signalling. Oncogene *27*, 966–975.

Chua, A.C., Klopcic, B., Lawrance, I.C., Olynyk, J.K., and Trinder, D. (2010). Iron: an emerging factor in colorectal carcinogenesis. World J. Gastroenterol. *16*, 663–672.

de Alboran, I.M., O'Hagan, R.C., Gärtner, F., Malynn, B., Davidson, L., Rickert, R., Rajewsky, K., DePinho, R.A., and Alt, F.W. (2001). Analysis of C-MYC function in normal cells via conditional gene-targeted mutation. Immunity *14*, 45–55.

de Lau, W., Barker, N., Low, T.Y., Koo, B.K., Li, V.S., Teunissen, H., Kujala, P., Haegebarth, A., Peters, P.J., van de Wetering, M., et al. (2011). Lgr5 homologues associate with Wnt receptors and mediate R-spondin signalling. Nature *476*, 293–297.

Edgren, G., Reilly, M., Hjalgrim, H., Tran, T.N., Rostgaard, K., Adami, J., Titlestad, K., Shanwell, A., Melbye, M., and Nyrén, O. (2008). Donation frequency, iron loss, and risk of cancer among blood donors. J. Natl. Cancer Inst. *100*, 572–579.

Ireland, H., Kemp, R., Houghton, C., Howard, L., Clarke, A.R., Sansom, O.J., and Winton, D.J. (2004). Inducible Cre-mediated control of gene expression in the murine gastrointestinal tract: effect of loss of beta-catenin. Gastroenterology *126*, 1236–1246.

Kato, I., Dnistrian, A.M., Schwartz, M., Toniolo, P., Koenig, K., Shore, R.E., Zeleniuch-Jacquotte, A., Akhmedkhanov, A., and Riboli, E. (1999). Iron intake, body iron stores and colorectal cancer risk in women: a nested case-control study. Int. J. Cancer *80*, 693–698.

Le, N.T., and Richardson, D.R. (2002). The role of iron in cell cycle progression and the proliferation of neoplastic cells. Biochim. Biophys. Acta *1603*, 31–46.

Lee, D.H., Anderson, K.E., Harnack, L.J., Folsom, A.R., and Jacobs, D.R., Jr. (2004). Heme iron, zinc, alcohol consumption, and colon cancer: Iowa Women's Health Study. J. Natl. Cancer Inst. *96*, 403–407.

Lewis, A., Segditsas, S., Deheragoda, M., Pollard, P., Jeffery, R., Nye, E., Lockstone, H., Davis, H., Clark, S., Stamp, G., et al. (2010). Severe polyposis in Apc(1322T) mice is associated with submaximal Wnt signalling and increased expression of the stem cell marker Lgr5. Gut *59*, 1680–1686.

Littlewood, T.D., Hancock, D.C., Danielian, P.S., Parker, M.G., and Evan, G.I. (1995). A modified oestrogen receptor ligand-binding domain as an improved switch for the regulation of heterologous proteins. Nucleic Acids Res. *23*, 1686–1690.

Lund, E.K., Wharf, S.G., Fairweather-Tait, S.J., and Johnson, I.T. (1998). Increases in the concentrations of available iron in response to dietary iron supplementation are associated with changes in crypt cell proliferation in rat large intestine. J. Nutr. *128*, 175–179.

Mainous, A.G., 3rd, Gill, J.M., and Everett, C.J. (2005). Transferrin saturation, dietary iron intake, and risk of cancer. Ann. Fam. Med. *3*, 131–137.

Merlos-Suárez, A., Barriga, F.M., Jung, P., Iglesias, M., Céspedes, M.V., Rossell, D., Sevillano, M., Hernando-Momblona, X., da Silva-Diz, V., Muñoz, P., et al. (2011). The intestinal stem cell signature identifies colorectal cancer stem cells and predicts disease relapse. Cell Stem Cell *8*, 511–524.

Nelson, R.L. (2001). Iron and colorectal cancer risk: human studies. Nutr. Rev. *59*, 140–148.

Nelson, R.L., Davis, F.G., Persky, V., and Becker, E. (1995). Risk of neoplastic and other diseases among people with heterozygosity for hereditary hemochromatosis. Cancer *76*, 875–879.

O'Donnell, K.A., Yu, D., Zeller, K.I., Kim, J.W., Racke, F., Thomas-Tikhonenko, A., and Dang, C.V. (2006). Activation of transferrin receptor 1 by c-Myc enhances cellular proliferation and tumorigenesis. Mol. Cell. Biol. *26*, 2373–2386.

Pigeon, C., Turlin, B., Iancu, T.C., Leroyer, P., Le Lan, J., Deugnier, Y., Brissot, P., and Loréal, O. (1999). Carbonyl-iron supplementation induces hepatocyte nuclear changes in BALB/CJ male mice. J. Hepatol. *30*, 926–934.

Pollard, P., Deheragoda, M., Segditsas, S., Lewis, A., Rowan, A., Howarth, K., Willis, L., Nye, E., McCart, A., Mandir, N., et al. (2009). The Apc 1322T mouse develops severe polyposis associated with submaximal nuclear beta-catenin expression. Gastroenterology *136*, 2204–2213.

Potter, S.S., and Brunskill, E.W. (2012). Laser capture. Methods Mol. Biol. *886*, 211–221.

Sansom, O.J., Reed, K.R., Hayes, A.J., Ireland, H., Brinkmann, H., Newton, I.P., Batlle, E., Simon-Assmann, P., Clevers, H., Nathke, I.S., et al. (2004). Loss of Apc in vivo immediately perturbs Wnt signaling, differentiation, and migration. Genes Dev. *18*, 1385–1390.

Sansom, O.J., Meniel, V.S., Muncan, V., Phesse, T.J., Wilkins, J.A., Reed, K.R., Vass, J.K., Athineos, D., Clevers, H., and Clarke, A.R. (2007). Myc deletion rescues Apc deficiency in the small intestine. Nature *446*, 676–679.

Shaheen, N.J., Silverman, L.M., Keku, T., Lawrence, L.B., Rohlfs, E.M., Martin, C.F., Galanko, J., and Sandler, R.S. (2003). Association between hemochromatosis (HFE) gene mutation carrier status and the risk of colon cancer. J. Natl. Cancer Inst. *95*, 154–159.

Shibata, H., Toyama, K., Shioya, H., Ito, M., Hirota, M., Hasegawa, S., Matsumoto, H., Takano, H., Akiyama, T., Toyoshima, K., et al. (1997). Rapid colorectal adenoma formation initiated by conditional targeting of the Apc gene. Science *278*, 120–123.

Song, S., Christova, T., Perusini, S., Alizadeh, S., Bao, R.Y., Miller, B.W., Hurren, R., Jitkova, Y., Gronda, M., Isaac, M., et al. (2011). Wnt inhibitor screen reveals iron dependence of β-catenin signaling in cancers. Cancer Res. *71*, 7628–7639.

Soyars, K.E., and Fischer, J.G. (1998). Iron supplementation does not affect cell proliferation or aberrant crypt foci development in the colon of Sprague-Dawley rats. J. Nutr. *128*, 764–770.

Su, L.K., Kinzler, K.W., Vogelstein, B., Preisinger, A.C., Moser, A.R., Luongo, C., Gould, K.A., and Dove, W.F. (1992). Multiple intestinal neoplasia caused by a mutation in the murine homolog of the APC gene. Science *256*, 668–670.

Theurl, I., Ludwiczek, S., Eller, P., Seifert, M., Artner, E., Brunner, P., and Weiss, G. (2005). Pathways for the regulation of body iron homeostasis in response to experimental iron overload. J. Hepatol. *43*, 711–719.

Toyokuni, S. (1996). Iron-induced carcinogenesis: the role of redox regulation. Free Radic. Biol. Med. *20*, 553–566.

Toyokuni, S. (2009). Role of iron in carcinogenesis: cancer as a ferrotoxic disease. Cancer Sci. *100*, 9–16.

van der Flier, L.G., Sabates-Bellver, J., Oving, I., Haegebarth, A., De Palo, M., Anti, M., van Gijn, M.E., Suijkerbuijk, S., van de Wetering, M., Marra, G., and

Clevers, H. (2007). The intestinal Wnt/TCF signature. Gastroenterology *132*, 628–632.

van der Flier, L.G., van Gijn, M.E., Hatzis, P., Kujala, P., Haegebarth, A., Stange, D.E., Begthel, H., van den Born, M., Guryev, V., Oving, I., et al. (2009). Transcription factor achaete scute-like 2 controls intestinal stem cell fate. Cell *136*, 903–912.

Ward, D.G., Roberts, K., Brookes, M.J., Joy, H., Martin, A., Ismail, T., Spychal, R., Iqbal, T., and Tselepis, C. (2008). Increased hepcidin expression in colorectal carcinogenesis. World J. Gastroenterol. *14*, 1339–1345.

Weinberg, E.D. (1994). Association of iron with colorectal cancer. Biometals *7*, 211–216.

Weinberg, E.D. (1996). The role of iron in cancer. Eur. J. Cancer Prev. *5*, 19–36.

Whitnall, M., Howard, J., Ponka, P., and Richardson, D.R. (2006). A class of iron chelators with a wide spectrum of potent antitumor activity that overcomes resistance to chemotherapeutics. Proc. Natl. Acad. Sci. USA *103*, 14901–14906.

World Cancer Research Fund / American Institute for Cancer Research. (2011). Continuous Update Project Interim Report Summary (Food, Nutrition, Physical Activity, and the Prevention of Colorectal Cancer).

Wu, K.J., Polack, A., and Dalla-Favera, R. (1999). Coordinated regulation of iron-controlling genes, H-ferritin and IRP2, by c-MYC. Science *283*, 676–679.

Zacharski, L.R., Chow, B.K., Howes, P.S., Shamayeva, G., Baron, J.A., Dalman, R.L., Malenka, D.J., Ozaki, C.K., and Lavori, P.W. (2008). Decreased cancer risk after iron reduction in patients with peripheral arterial disease: results from a randomized trial. J. Natl. Cancer Inst. *100*, 996–1002.